ARCHIWUM ENERGETYKI tom XLIII(2013), nr 1-2, 129–146

Andrzej Rusin*
Marian Lipka
Henryk Łukowicz

Silesian University of Technology
Institute of Power Engineering and Turbomachinery
Gliwice

Thermal and stress states in unsteady conditions of operation of the rotors of ultra-supercritical parameter turbines

The paper presents the results of numerical analyses, including the steam turbine rotor, for a newly designed 900 MW power unit with ultra-supercritical steam parameters (650 °C, 30.0 MPa). With the use of preliminary design calculations and assuming the optimum structural solutions, simulations of the turbine operation in unsteady conditions are carried out. The analyses take account of the turbine start-up from the different thermal states, i.e., the cold, warm and hot states, and with different rates of increment in the steam parameters. The maps of the temperature field and the stress distributions are obtained. Based on them, the areas with the highest level of stress are identified, i.e., the rotor critical areas which have a direct impact on the life of the entire machine. The performed simulations and analyses make it possible, already at the design stage, to determine the ranges of possible values of stress amplitudes occurring in the main components of the turbine. This in turn allows a preliminary assessment of the turbine life.

1 Introduction

The new trends in the development of professional coal-based power engineering tend to a further increase in the steam parameters. This entails the need to search for new design solutions, among others in turbine construction, and to select such materials that will satisfy the requirement of safe operation of turbines. The first stage in this kind of research is the preliminary optimisation

*Corresponding Author. E-mail: andrzej.rusin@polsl.pl

of the new-generation rotors shape. Based on the power unit thermal cycle calculations, a preliminary structural form of the high pressure (HP) part rotor is developed and then the areas with the highest level of stress are optimised. The full reaction rotor is assumed as the initial one. The following elements among others, are optimised: the blade groove shapes, the rotor curvature radii and the shapes of the shaft internal chambers. In each case, the obtained solutions result in a more advantageous stress level compared to the initial one [1]. The next optimisation stage concerns the improvement in the operation flexibility and comprises the development of the turbine start-up characteristics. The start-up characteristics are developed for three basic types of start-up: from the cold, warm and hot states. Three variants are developed in each case, with an average rate of the increase in the live steam temperature of 1.5 K/min, 2.0 K/min and 2.5 K/min, respectively. The characteristics include the temperature and the live steam pressure curves, as well as, the curves of the mass flow and the rotor revolutions. For each characteristic, analyses are performed of the distributions of the temperature fields and of the equivalent (von Mises) stress and its components in the high pressure turbine rotor. Additionally, in each of the cases mentioned above the impact of the component initial thermal state on the stress state during start-up is examined. The rotor areas with the highest stress are identified.

2 The geometrical and material model of the turbine high pressure part rotor

The full reaction rotor is the subject of the design optimisation process [1,2]. As a result, a rotor model is obtained with a geometry as presented in Fig. 1. Additionally, an enlarged fragment of the model is shown that comprises the area of the groove of the seventh stage (Fig. 2).

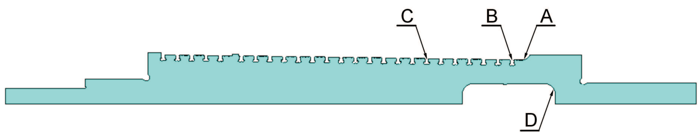

Figure 1. Model of the optimised rotor of the turbine high pressure part.

In Fig. 1 four areas are pointed out (A, B, C, and D critical areas under analysis) which feature the highest level of stress during the preliminary analyses on the model. These areas, referred to as critical, comprise:

- bottom of the first thermal groove (area A),

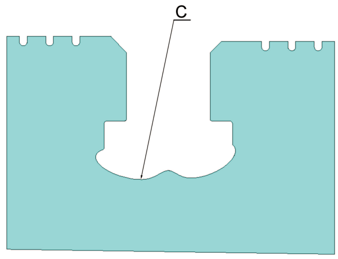

Figure 2. The seventh stage groove of the optimised rotor of the turbine high pressure part.

- bottom of the groove of the first blade stage (area B),
- bottom of the groove of the seventh blade stage (area C),
- corner of the internal chamber (area D).

It is assumed that the turbine components are made of chromium steel (9–12% Cr), with properties varying in the range of temperatures from 200 to 650 °C [3,4]. These properties are assumed partially based on own studies carried out for a rotor steel forging [2,5]. An example change in the Young's modulus value depending on temperature is presented in Fig. 3.

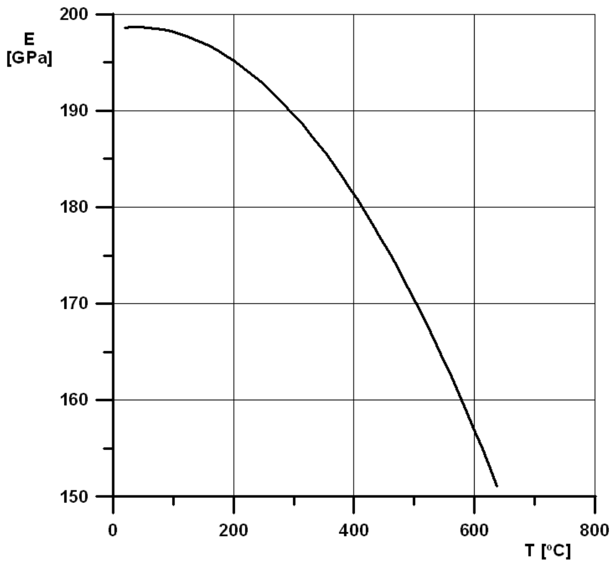

Figure 3. Change in Young' modulus, E, depending on temperature, T.

3 Unsteady thermal and strength states in the optimised rotor of the turbine high pressure part

Taking account of the thermal and flow calculations of the turbine and the calculations of the entire cycle, a family of the turbine start-up characteristics are developed. For this purpose it is assumed that [2]:

- there is a slide pressure adjustment of live steam in the boiler,
- operation with slide pressure occurs in the 40–100% range of load,
- pressure of reheated steam for loads included in the range from 0 to 40% is maintained at a constant level by means of an (intermediate–low pressure) IP–LP bypass station and a valve before the intermediate pressure (IP) part (the pressure value should result from the conditions of the steam reheater cooling, and the bypass of the HP part is closed at the 40% load).

The start-ups from the initial cold, warm and hot states of the turbine are analysed. It is assumed that according to the reference characteristic the start-up is run with the average steam temperature increment rate of $\Delta T/\Delta t = 2.0$ K/min (here ΔT and Δt denote temperature and time increments, respectively). Subsequent characteristics describe a slower start-up of the turbine – at the rate of $\Delta T/\Delta t = 1.5$ K/min – and an accelerated process – at the rate of $\Delta T/\Delta t = 2.5$ K/min.

The numerical analyses of unsteady states were conducted in two variants. The first group of calculations comprises start-ups assuming that $\Delta T_{s-m} = 0$ K, i.e., there is no initial difference between the temperature of steam flowing onto the first stage and the temperature of the metal. For the other group of calculations it is assumed that the temperature of the flowing steam is by 50 K higher than the initial temperature of the metal ($\Delta T_{s-m} = 50$ K). The aim of such simulations is to find the impact of the initial difference in temperature on the thermal and stress state of the turbine rotor [5].

The thermal boundary conditions and the pressure distribution on the surface of the components are assumed based on the results of the calculations performed using the dependencies and procedures developed at the Institute of Power Engineering and Turbomachinery in Gliwice [6].

3.1 Start-up from the initial cold state with the average rate of the live steam temperature increment of $\Delta T/\Delta t = 2.0$ K/min

The simulation of start-up from the initial cold state runs according to the dependencies shown in the start-up characteristic (Fig. 4.). It is assumed that the

$\Delta T/\Delta t$ gradient of the live steam temperature increment is 2.0 K/min. The initial live steam temperature is assumed at 320 °C. The turbine reaches the nominal parameters about 200 min after start-up. The curves illustrating the

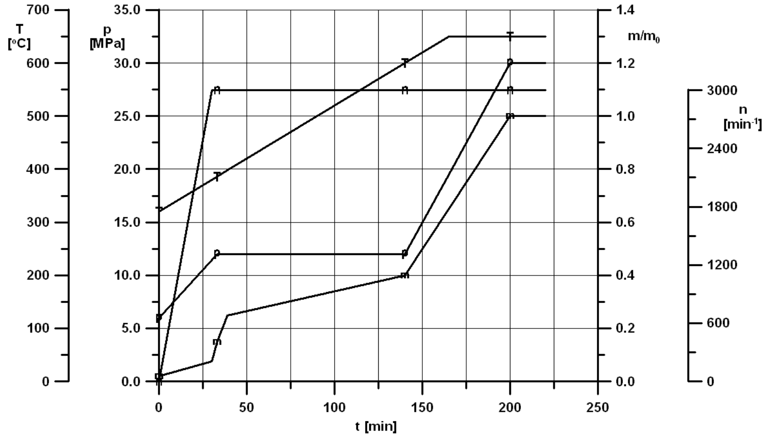

Figure 4. The characteristic of the power unit start-up from the initial cold state for the live steam temperature increment $\Delta T/\Delta t = 2.0$ K/min (T – live steam temperature, p – live steam pressure, n – rotor revolutions, m/m_o – turbine driving steam flow to the nominal steam flow ratio).

changes in temperatures and equivalent (von Mises) stress in the rotor critical areas (shown in Figs. 1 and 2) are presented in Figs. 5 and 6.

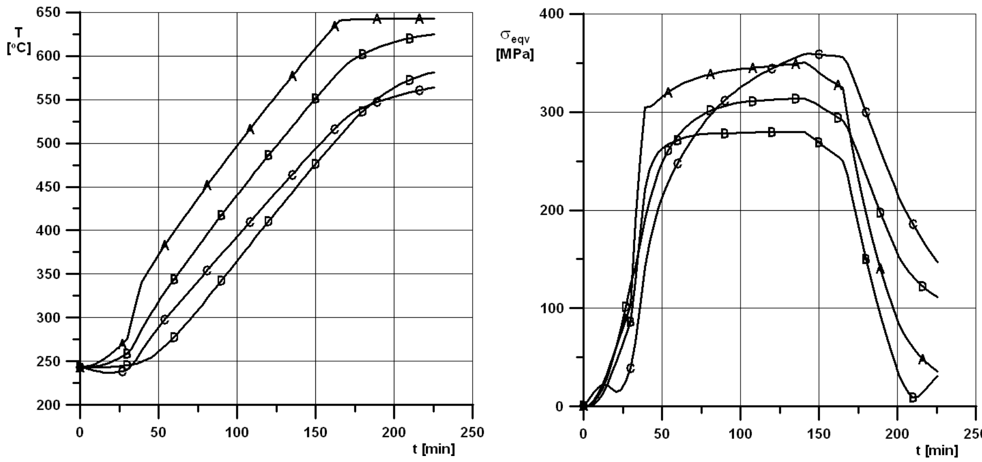

Figure 5. The curves illustrating the changes in the metal temperatures (T) and in the equivalent (von Mises) stress (σ_{eqv}) in the critical areas (A,B,C, and D) of the rotor of the turbine HP part for $\Delta T_{s-m} = 0$ K.

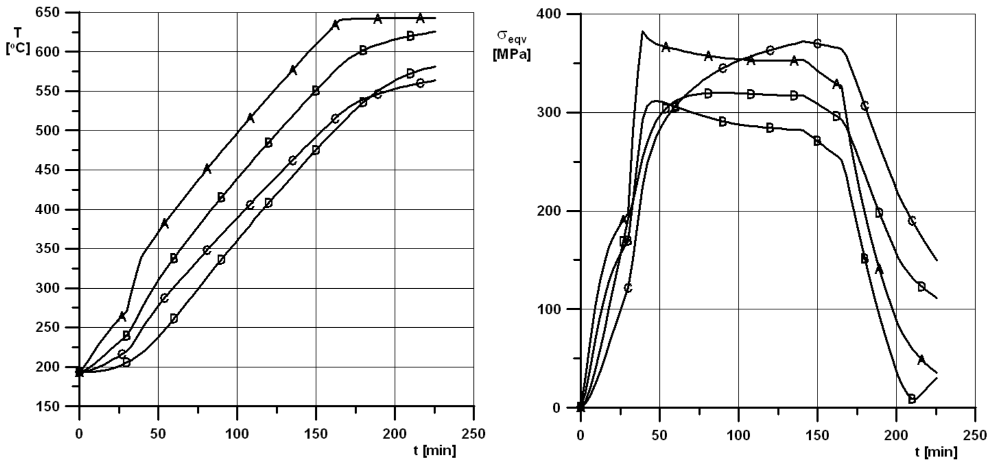

Figure 6. The curves illustrating the changes in the metal temperatures and in the equivalent (von Mises) stress in the critical areas (A,B,C, and D) of the rotor of the turbine HP part for $\Delta T_{s-m} = 50$ K.

The Figs. 7–12 present the maps of the distributions of temperature fields and of the values of equivalent (von Mises) stress for the start-up at $\Delta T_{s-m} = 50$ K at the moment when maximum values of stress appear, i.e., in the 39th minute of the process.

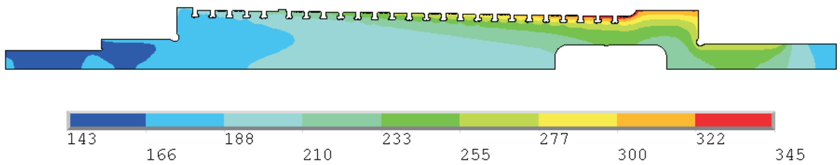

Figure 7. Temperature distribution in the rotor of the turbine HP part in the 39th minute of the start-up process for $\Delta T_{s-m} = 50$ K.

3.2 Start-up from the initial cold state with the average rate of the live steam temperature increment of $\Delta T/\Delta t = 1.5$ K/min

The next start-up from the initial cold state was conducted with a lower rate of the live steam temperature increment ($\Delta T/\Delta t = 1.5$ K/min). The start-up characteristic is shown in Fig. 13. The same live steam initial temperature (320 °C) is assumed as in the previous case. The turbine reaches its nominal parameters about 270 min after start-up. The curves illustrating the changes in temperatures and in the equivalent (von Mises) stress in the rotor critical areas are presented in Figs. 14 and 15.

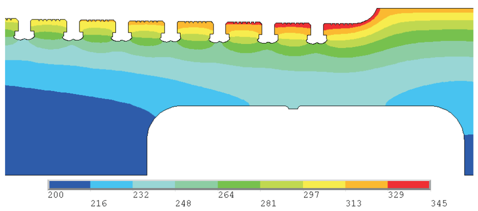

Figure 8. Temperature distribution in the first seven stages of the rotor of the turbine HP part in the 39th minute of the start-up process for $\Delta T_{s-m} = 50$ K.

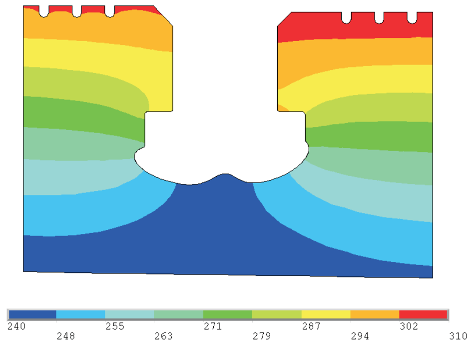

Figure 9. Temperature distribution in the groove area of the seventh stage of the rotor of the turbine HP part in the 39th minute of the start-up process for $\Delta T_{s-m} = 50$ K.

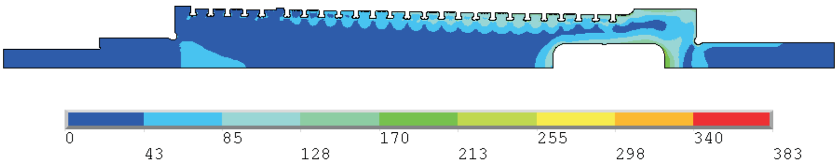

Figure 10. Distribution of equivalent (von Mises) stress in the rotor of the turbine HP part in the 39th minute of the start-up process for $\Delta T_{s-m} = 50$ K.

3.3 Start-up from the initial cold state with the average rate of the live steam temperature increment of $\Delta T/\Delta t = 2.5$ K/min

The last in the simulation series of start-ups from the initial cold state comprises an accelerated process with the rate of the live steam temperature increment of $\Delta T/\Delta t = 2.5$ K/min. The start-up itself is performed according to the dependencies shown in Fig. 16. The initial live steam temperature is 320 °C. The steam nominal parameters stabilise about 162 min after start-up. The nature of the changes in the metal temperatures and in the equivalent (von Mises) stress in the analysed areas of the rotor (A, B, C, and D) are presented in Figs. 17 and 18.

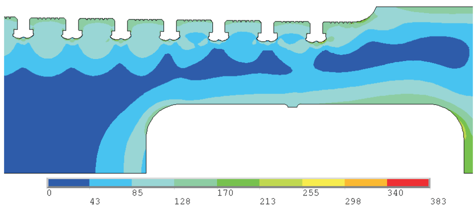

Figure 11. Distribution of equivalent (von Mises) stress in the area of the first seven stages of the rotor of the turbine HP part in the 39th minute of the start-up process for $\Delta T_{s-m} = 50$ K.

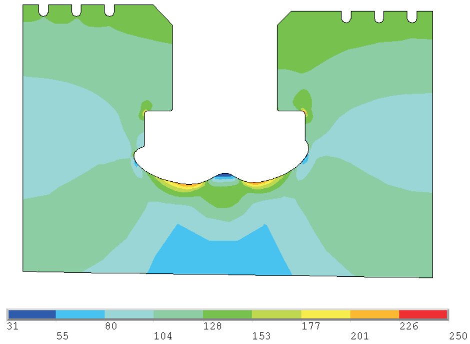

Figure 12. Distribution of equivalent (von Mises) stress in the groove area of the seventh stage of the rotor of the turbine HP part in the 39th minute of the start-up process for $\Delta T_{s-m} = 50$ K.

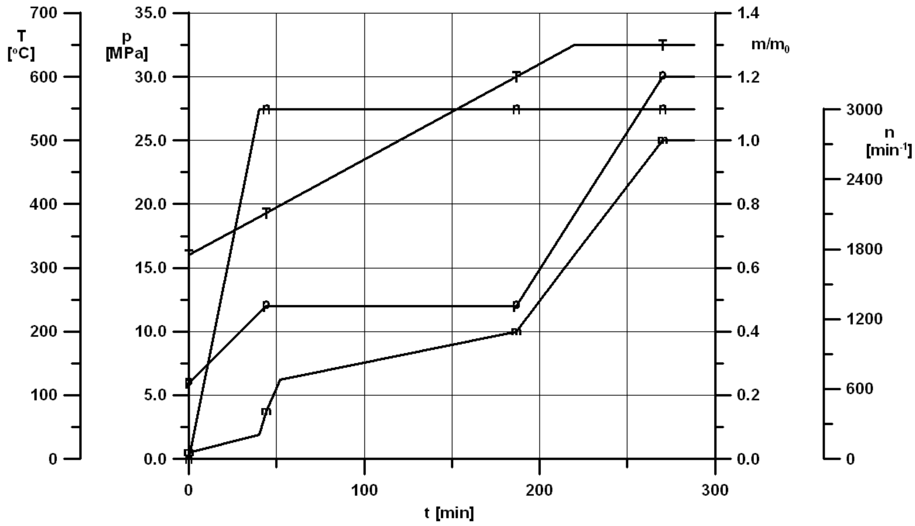

Figure 13. The characteristic of the power unit start-up from the initial cold state for the live steam temperature increment $\Delta T_{s-m} = 1.5$ K.

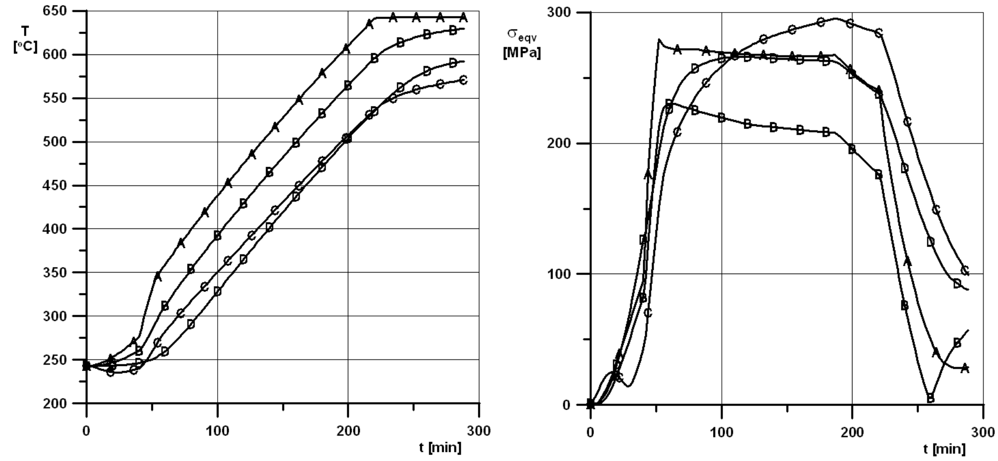

Figure 14. The curves illustrating the changes in the metal temperatures and in the equivalent (von Mises) stress in the critical areas (A,B,C, and D) of the rotor of the turbine HP part for $\Delta T_{s-m} = 0$ K.

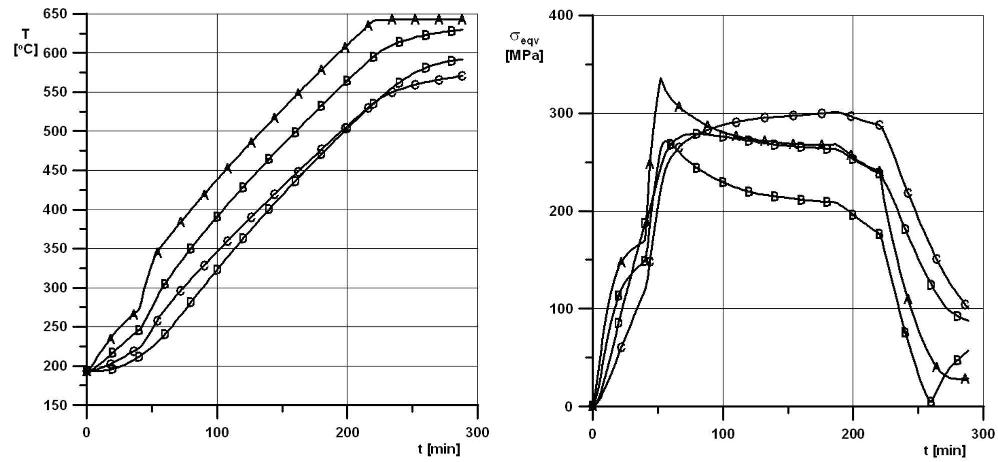

Figure 15. The curves illustrating the changes in the metal temperatures and in the equivalent (von Mises) stress in the critical areas (A,B,C, and D) of the rotor of the turbine HP part for $\Delta T_{s-m} = 50$ K.

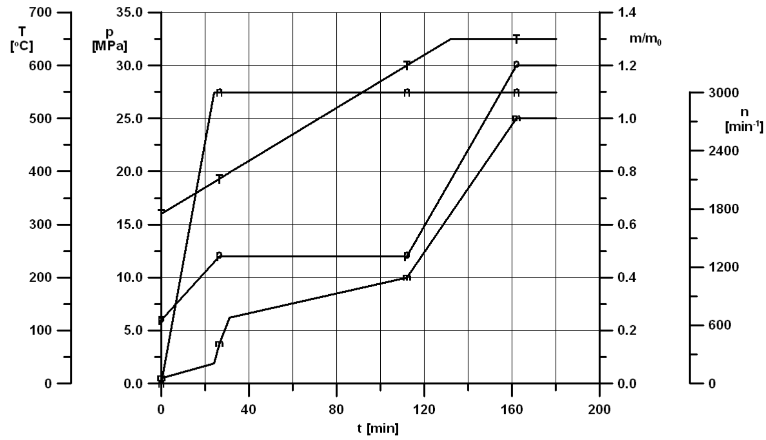

Figure 16. The characteristic of the power unit start-up from the initial cold state for the live steam temperature increment $\Delta T_{s-m} = 2.5$ K.

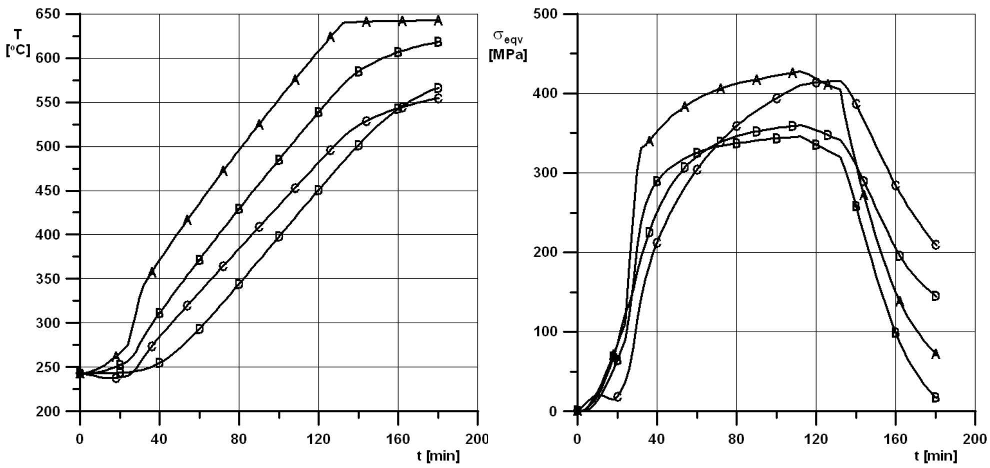

Figure 17. The curves illustrating the changes in the metal temperatures and in the equivalent (von Mises) stress in the critical areas (A,B,C, and D) of the rotor of the turbine HP part for $\Delta T_{s-m} = 0$ K.

3.4 Start-up from the initial warm state with the average rate of the live steam temperature increment of $\Delta T/\Delta t = 2.0$ K/min

Similarly to start-up from the initial cold state, the start-up from the initial warm state are also simulated for all the three rates of increment in the live steam temperature mentioned above. In this part, however, the results of the analyses

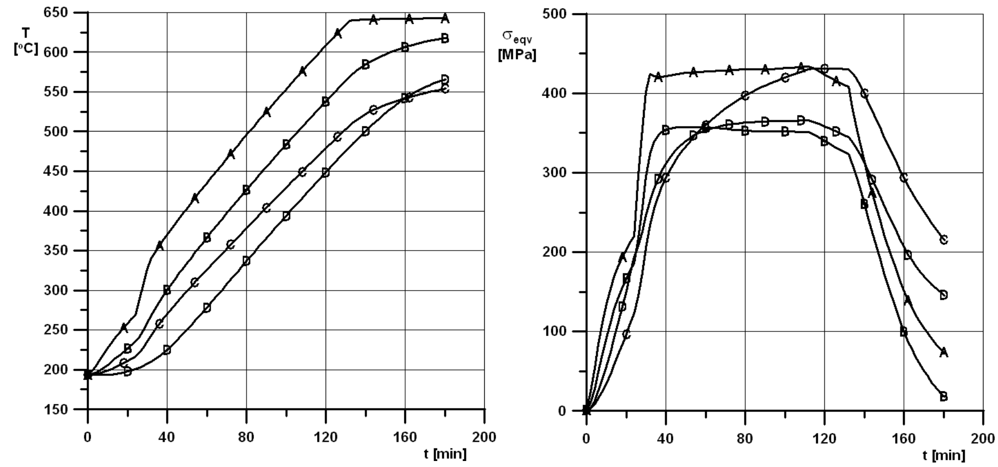

Figure 18. The curves illustrating the changes in the metal temperatures and in the equivalent (von Mises) stress in the critical areas (A,B,C, and D) of the rotor of the turbine HP part for $\Delta T_{s-m} = 50$ K.

are presented for the reference characteristic, i.e., for $\Delta T/\Delta t = 2.0$ K/min. The start-up is modelled according to the curves shown in Fig. 19. The initial live steam temperature is 480 °C. The turbine reaches the nominal parameters of the working agent about 100 min. after the process begins. The curves illustrating

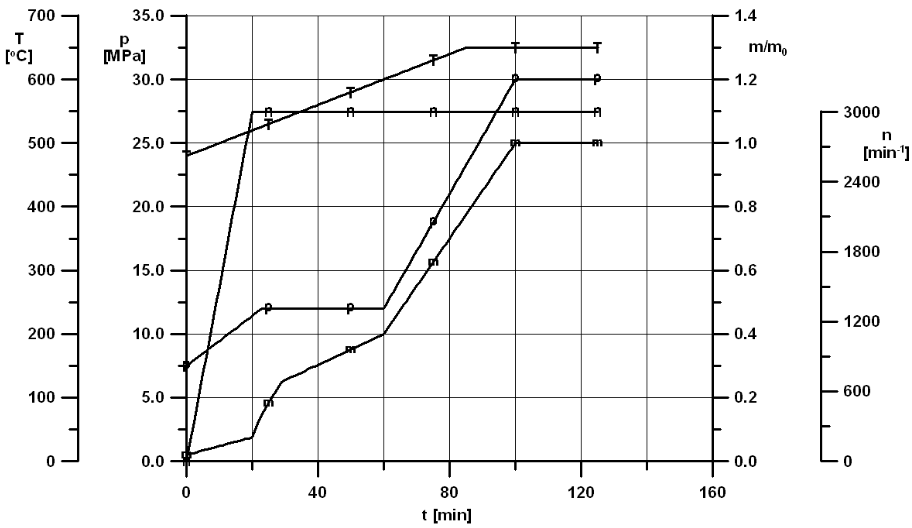

Figure 19. The characteristic of the power unit start-up from the initial warm state for the live steam temperature increment $\Delta T/\Delta t = 2.0$ K.

the changes in the metal temperatures and in the equivalent (von Mises) stress in the rotor critical areas (A, B, C, and D) are presented in Figs. 20 and 21.

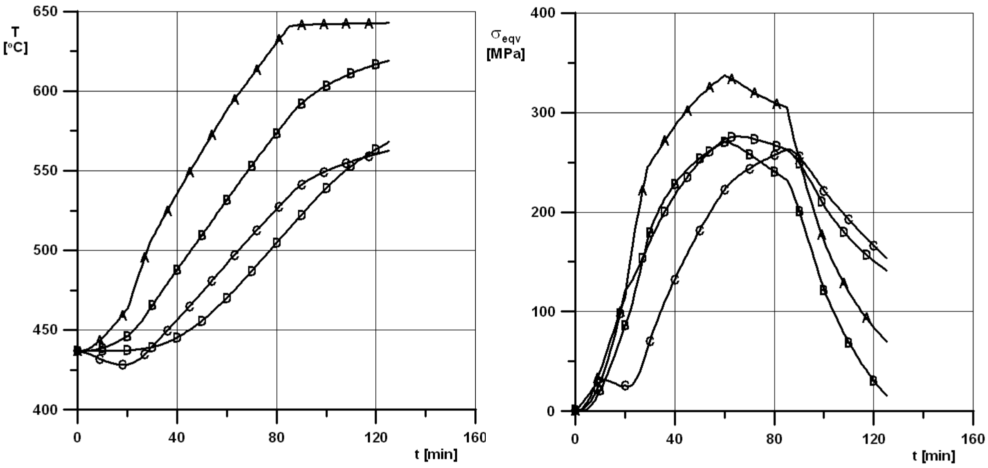

Figure 20. The curves illustrating the changes in the metal temperatures and in the equivalent (von Mises) stress in the critical areas (A,B,C, and D) of the rotor of the turbine HP part for $\Delta T_{sm} = 0$ K.

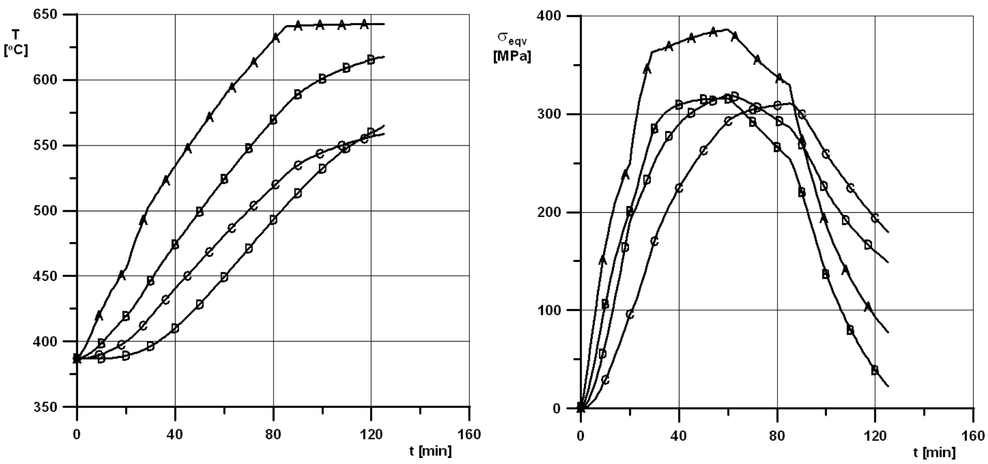

Figure 21. The curves illustrating the changes in the metal temperatures and in the equivalent (von Mises) stress in the critical areas (A,B,C, and D) of the rotor of the turbine HP part for $\Delta T_{sm} = 50$ K.

3.5 Start-up from the initial hot state with the average rate of the live steam temperature increment of $\Delta T/\Delta t = 2.0$ K/min

The analysis of start-up from the initial hot state was conducted according to the dependencies shown in the start-up characteristic (Fig. 22.). It was assumed that the $\Delta T/\Delta t$ gradient of the live steam temperature increment is 2.0 K/min. The initial live steam temperature is 550 °C. The steam nominal parameters stabilise about 75 min after start-up.

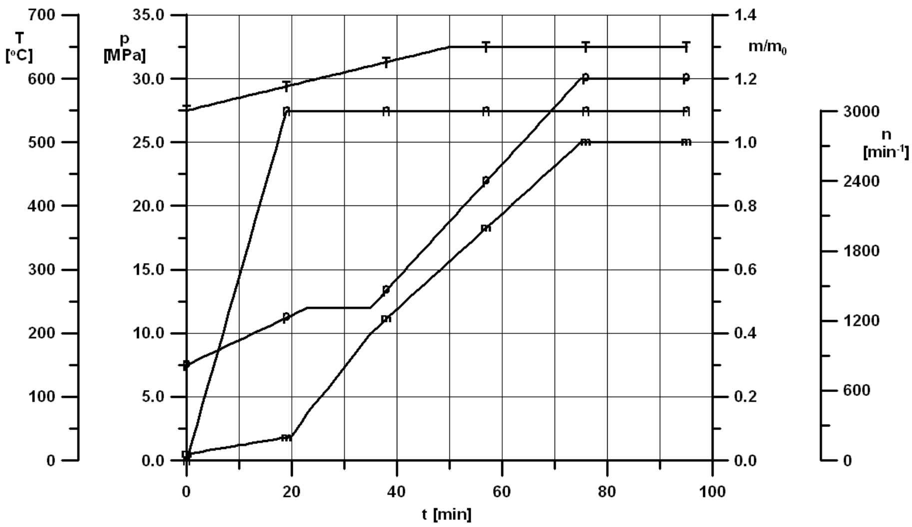

Figure 22. The characteristic of the power unit start-up from the initial hot state for the live steam temperature increment $\Delta T/\Delta t = 2.0$ K.

The range of the changes in the metal temperatures and in equivalent (von Mises) stress during start-up in the rotor critical areas are presented in Figs. 23 and 24.

4 Conclusions

Based on the performed calculations, the values of maximum stress in selected areas (A,B,C, and D) of the rotor which occur during start-up from different initial states are compared. These results are listed in Tabs. 1–4.

The new generations of currently designed power units feature a very high electricity generation efficiency which is achieved, among others, using ultra-supercritical steam parameters. At the same time, there appear problems related

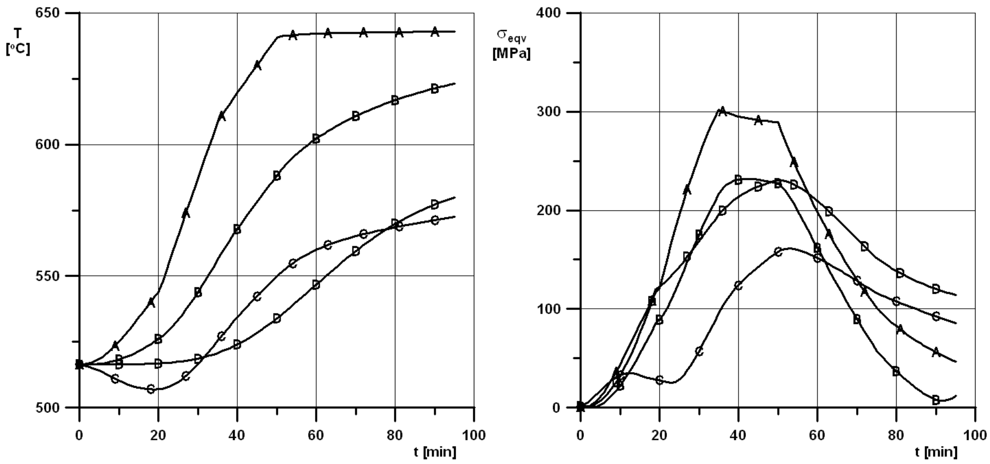

Figure 23. The curves illustrating the changes in the metal temperatures and in the equivalent (von Mises) stress in the critical areas (A,B,C, and D) of the rotor of the turbine HP part for $\Delta T_{sm} = 0$ K.

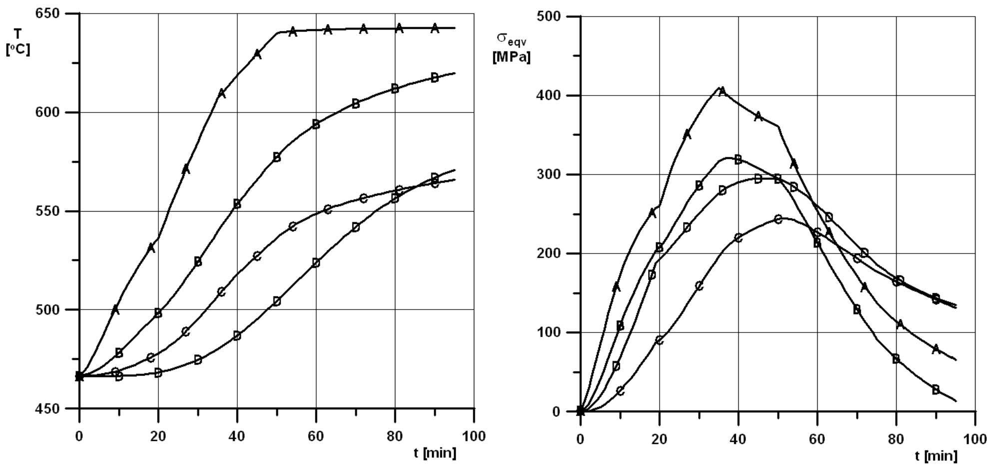

Figure 24. The curves illustrating the changes in the metal temperatures and in the equivalent (von Mises) stress in the critical areas (A,B,C, and D) of the rotor of the turbine HP part for $\Delta T_{sm} = 50$ K.

to the appropriate selection of materials used to make machine components and equipment. The selection of the material for the turbine rotors, especially of the HP and IP parts, poses a special problem. Literature findings [3,4] and the (rather limited) operational experience gained so far indicate that steels with a content of 9–12% of Cr may be successfully used to make rotors of such turbines. It is also obvious that a further increase in the steam parameters to the level of

Table 1. Maximum stress in the A area of the rotor.

The rotor initial state	$\Delta T/\Delta t$ [K/min]	ΔT_{s-m} [K]	$\sigma_{eqv,max}$ [MPa]	Time of occurence [min]
Cold	2.0	0	350.5	141
Cold	1.5	0	279.8	52
Cold	2.5	0	427.7	112
Cold	2.0	50	382.6	39
Cold	1.5	50	336.2	52
Cold	2.5	50	434.2	112
Warm	2.0	0	337.2	60
Warm	1.5	0	276.3	80
Warm	2.5	0	382.9	48
Warm	2.0	50	386.4	60
Warm	1.5	50	323.4	35
Warm	2.5	50	448.8	48
Hot	2.0	0	302.2	35
Hot	2.0	50	409.6	35

Table 2. Maximum stress in the B area of the rotor.

The rotor initial state	$\Delta T/\Delta t$ [K/min]	ΔT_{s-m} [K]	$\sigma_{eqv,max}$ [MPa]	Time of occurence [min]
Cold	2.0	0	279.6	120
Cold	1.5	0	230.2	62
Cold	2.5	0	345.6	112
Cold	2.0	50	311.8	48
Cold	1.5	50	271.6	56
Cold	2.5	50	357.5	50
Warm	2.0	0	270.3	60
Warm	1.5	0	219.9	80
Warm	2.5	0	307.0	50
Warm	2.0	50	315.6	56
Warm	1.5	50	264.0	44
Warm	2.5	50	367.4	48
Hot	2.0	0	231.8	42
Hot	2.0	50	320.9	38

700 °C calls for the use of nickel superalloys. It is not yet fully settled whether chromium steels could be used to operate in the temperature of about 650 °C. The analysed unsteady states of the turbine operation reveal the levels of stress that might appear in rotors. Comparing these results with own studies of steel X12CrMoWVNbN10, it may be concluded that practically in all the cases under analysis the maximum values of equivalent (von Mises) stress (449 MPa) do not

Table 3. Maximum stress in the C area of the rotor.

The rotor initial state	$\Delta T/\Delta t$ [K/min]	ΔT_{s-m} [K]	$\sigma_{eqv,max}$ [MPa]	Time of occurence [min]
Cold	2.0	0	359.5	147
Cold	1.5	0	295.1	186
Cold	2.5	0	415.8	132
Cold	2.0	50	372.1	141
Cold	1.5	50	301.2	186
Cold	2.5	50	431.5	118
Warm	2.0	0	262.9	86
Warm	1.5	0	232.0	113
Warm	2.5	0	310.6	85
Warm	2.0	50	268.7	86
Warm	1.5	50	342.0	68
Warm	2.5	50	161.3	53
Hot	2.0	0	244.7	51
Hot	2.0	50	409.6	35

Table 4. Maximum stress in the D area of the rotor.

The rotor initial state	$\Delta T/\Delta t$ [K/min]	ΔT_{s-m} [K]	$\sigma_{eqv,max}$ [MPa]	Time of occurence [min]
Cold	2.0	0	313.9	141
Cold	1.5	0	266.1	116
Cold	2.5	0	359.9	112
Cold	2.0	50	319.9	90
Cold	1.5	50	279.0	78
Cold	2.5	50	366.1	112
Warm	2.0	0	275.9	65
Warm	1.5	0	250.4	81
Warm	2.5	0	295.3	59
Warm	2.0	50	319.1	60
Warm	1.5	50	279.6	74
Warm	2.5	50	345.1	51
Hot	2.0	0	230.3	50
Hot	2.0	50	295.1	47

exceed the yield stress value (600 MPa), which proves that it is possible to use this steel and that this kind of steel features sufficient mechanical properties. An issue which needs further research is a more detailed determination of the creep properties of these particular steel grades.

Acknowledgement The results presented in this paper were obtained from research work co-financed by the National Centre of Research and Development in the framework of Contract SP/E/1/67484/10 – Strategic Research Programme – Advanced technologies for energy generation: "Development of a technology for highly efficient 'zero-emission' coal-fired power units integrated with CO_2 capture".

Received in September 2012

References

[1] Rusin A., Lipka M., Łukowicz H.: *Selected aspects of a preliminary design of rotors of ultra-supercritical parameter turbines.* Kraftwerkstechnik, Siechere und nachhaltige Energieversorgung, Band 3, 43. Kraftwerkstechnisches Kolloquium. Dresden, 2011. Tagungsband 28.

[2] Rusin A., Lipka M., Łukowicz H., Bieniek M.: *Identifying Thermal and Strength States in New Generation Turbine Rotors.* Report on the completion of Stage 14 – III.1.1a of the Strategic Research Programme – 'Advanced technologies for obtaining energy' Task 1: 'Development of technologies for highly efficient zero-emission coal-fired power units integrated with CO2 capture from flue gases'. Gliwice 2011 (in Polish).

[3] Wang Y., Mayer K.H., Scholz A., Berger C., Chilukuru H., Durst K., Blum W.: *Development of new 11% Cr heat resistant ferritic steels with enhanced creep resistance for steam power plants with operating steam temperatures up to 650 °C.* Mat. Sci. Eng. A, 2009, 180-184.

[4] Viswanathan R., Coleman K., Rao U.: *Materials for ultra-supercritical coal-fired power plant boilers.* Int. J. Pressure Vessels and Piping **83**(2006), 778–783.

[5] Rusin A., Łukowicz H., Lipka M.: *Development of turbine start-up characteristics.* Report on the completion of Stage 17 – IV.2.3.2b of the Strategic Research Programme – 'Advanced technologies for obtaining energy' Task 1: 'Development of technologies for highly efficient zero-emission coal-fired power units integrated with CO_2 capture from flue gases'. Gliwice 2012 (in Polish).

[6] Łukowicz H.: *Analysis problems in flow calculations of steam turbines applied in diagnostics and design.* Zeszyty Naukowe Politechniki Śląskiej. Silesian University of Technology, Gliwice 2005 (in Polish).

Stany termiczne i wytrzymałościowe w nieustalonych warunkach pracy wirników turbin na parametry super-nadkrytyczne

S t r e s z c z e n i e

W pracy przedstawiono wyniki analiz numerycznych, obejmujących wirnik turbiny parowej dla nowoprojektowanego bloku o mocy 900 MW na parametry super-nadkrytyczne (650 °C, 30 MPa). Opierając sie na wcześniej przeprowadzonych obliczeniach projektowych, po przyjęciu

optymalnego rozwiązania konstrukcyjnego, przeprowadzono symulację pracy turbiny w warunkach nieustalonych. Analizy uwzględniały rozruchy turbiny zarówno z różnych początkowych stanów cieplnych, tj. zimnego, ciepłego oraz gorącego, jak i realizowanych z różnymi prędkościami przyrostu parametrów pary. Otrzymano mapy rozkładów pól temperatur oraz naprężeń. Na ich podstawie zidentyfikowano obszary o najwyższym poziomie wytężenia, tzn. obszary krytyczne wirnika, które w sposób bezpośredni będą wpływać na żywotność całej maszyny. Przeprowadzone symulacje i analizy pozwalają już na etapie prac projektowych określić zakresy możliwych wartości amplitud naprężeń występujących w głównych elementach turbiny. Pozwala to z kolei na wstępne oszacowanie trwałości turbiny.